Journal of the American College of Cardiology
© 2011 by the American College of Cardiology Foundation
Published by Elsevier Inc.

Vol. 57, No. 2, 2011
ISSN 0735-1097/$36.00
doi:10.1016/j.jacc.2010.07.043

Noninvasive Identification of Ventricular Tachycardia-Related Conducting Channels Using Contrast-Enhanced Magnetic Resonance Imaging in Patients With Chronic Myocardial Infarction

Comparison of Signal Intensity Scar Mapping and Endocardial Voltage Mapping

Esther Perez-David, MD,* Ángel Arenal, MD,* José L. Rubio-Guivernau, PHD,† Roberto del Castillo, MD,* Leonardo Atea, MD,* Elena Arbelo, MD, PHD,‡ Eduardo Caballero, MD, PHD,‡ Verónica Celorrio, MD,* Tomas Datino, MD, PHD,* Esteban Gonzalez-Torrecilla, MD, PHD,* Felipe Atienza, MD,* Maria J. Ledesma-Carbayo, PHD,† Javier Bermejo, MD,* Alfonso Medina, MD, PHD,‡ Francisco Fernández-Avilés, MD, PHD*

Madrid and Las Palmas de Gran Canaria, Spain

Objectives We performed noninvasive identification of post-infarction sustained monomorphic ventricular tachycardia (SMVT)–related slow conduction channels (CC) by contrast-enhanced magnetic resonance imaging (ceMRI).

Background Conduction channels identified by voltage mapping are the critical isthmuses of most SMVT. We hypothesized that CC are formed by heterogeneous tissue (HT) within the scar that can be detected by ceMRI.

Methods We studied 18 consecutive VT patients (SMVT group) and 18 patients matched for age, sex, infarct location, and left ventricular ejection fraction (control group). We used ceMRI to quantify the infarct size and differentiate it into scar core and HT based on signal-intensity (SI) thresholds (>3 SD and 2 to 3 SD greater than remote normal myocardium, respectively). Consecutive left ventricle slices were analyzed to determine the presence of continuous corridors of HT (channels) in the scar. In the SMVT group, color-coded shells displaying ceMRI subendocardial SI were generated (3-dimensional SI mapping) and compared with endocardial voltage maps.

Results No differences were observed between the 2 groups in myocardial, necrotic, or heterogeneous mass. The HT channels were more frequently observed in the SMVT group (88%) than in the control group (33%, $p < 0.001$). In the SMVT group, voltage mapping identified 26 CC in 17 of 18 patients. All CC corresponded, in location and orientation, to a similar channel detected by 3-dimensional SI mapping; 15 CC were related to 15 VT critical isthmuses.

Conclusions SMVT substrate can be identified by ceMRI scar heterogeneity analysis. This information could help identify patients at risk of VT and facilitate VT ablation. (J Am Coll Cardiol 2011;57:184–94) © 2011 by the American College of Cardiology Foundation

Human studies have demonstrated that the slow conduction areas of sustained monomorphic ventricular tachycardia (SMVT) re-entrant circuit are bundles of viable myocytes embedded in the scar tissue (1,2). These areas, which are bounded by compact scarred tissue, form conduction channels (CC) that can be identified during sinus rhythm by scar mapping of unexcitable areas during pacing (3) or endocardial voltage mapping (4,5).

See page 195

Contrast-enhanced magnetic resonance imaging (ceMRI) can accurately delineate the scar (6–8) and differentiate areas of lower signal intensity (SI) that contain viable myocytes, namely,

From the *Hospital General Universitario Gregorio Marañón, Madrid, Spain; †Universidad Politécnica de Madrid and CIBER-BBN, Madrid, Spain; and the ‡Hospital Universitario de Gran Canaria Dr. Negrín, Las Palmas de Gran Canaria, Spain. This study was partially supported by research projects TIN2007-68048-C02-01 and TIN2007-68048-C02-02 from the Spanish Ministry of Science and Innovation and Cooperative Cardiovascular Disease Research Network (RECAVA), Instituto de Salud Carlos III, Ministry of Health. Dr. Atienza is a consultant for Medtronic and has received a research grant from St. Jude's Medical, Spain. All other authors have reported that they have no relationships to disclose.

Manuscript received December 3, 2009; revised manuscript received June 25, 2010, accepted July 13, 2010.

heterogeneous tissue (HT) (9). The extension of HT correlates with increased cardiac mortality and VT inducibility (9,10). We also know that HT is not necessarily confined to the border of the infarct, and that it can be seen at more central locations (10), as occurs with CC (4).

We hypothesized that SMVT substrate are channels of HT that could be identified noninvasively by ceMRI. The purposes of the study were as follows: 1) to differentiate patients with and without spontaneous SMVT based on the presence or absence of HT channels; and 2) to identify CC by projecting the endocardial SI of ceMRI in a 3-dimensional (3D) endocardial shell.

Abbreviations and Acronyms

3D = 3-dimensional
CC = conduction channels
ceMRI = contrast-enhanced magnetic resonance imaging
HT = heterogeneous tissue
ICD = implantable cardioverter-defibrillator
MRI = magnetic resonance imaging
RF = radiofrequency
SI = signal intensity
SMVT = sustained monomorphic ventricular tachycardia
VT = ventricular tachycardia

Methods

Patients

SMVT group. We included 18 consecutive patients referred for ablation of SMVT who fulfilled the following inclusion criteria: 1) chronic myocardial infarction; 2) clinically documented SMVT; and 3) no contraindication for MRI, including the presence of an implantable cardioverter-defibrillator (ICD). All 18 patients with SMVT underwent clinical evaluation and MRI, followed by an electrophysiological study.

Control group. The SMVT group was compared with a control group selected from the MRI database. Participants were matched for age, sex, left ventricular ejection fraction, and infarct location, but did not have clinically documented VT, palpitation, or syncope. The study was performed according to local guidelines on ethics and methodology of clinical investigation. Informed consent was obtained from all participants.

MRI

Study and control patients underwent ceMRI with a 1.5-T scanner (Intera, Philips, Best, the Netherlands). A 5-element dedicated cardiac coil was used. All images were obtained with electrocardiogram gating and breath-holding.

The MRI study consisted of cine steady-state free-precession imaging of left ventricular function (SENSE × 2, repetition time: 2.4 ms, echo time: 1.2 ms, average in-plane spatial resolution: 1.6 × 2 mm, 30 phases per cycle, 8-mm slice thickness without gap) and late enhancement imaging of myocardial scar tissue (3D inversion-recovery turbo gradient echo sequence, pre-pulse delay optimized for maximal myocardial signal suppression; SENSE × 2, flip angle 15°, repetition time: 3.4 ms, echo time: 1.3 ms, actual spatial resolution: 1.48 × 1.66 mm, interpolated spatial resolution 1.29 × 1.29 mm, 5-mm actual slice thickness, inversion time: 200 to 300 ms; acquisition window was set to 150 to 170 ms and breath-holding length was 13 to 14 s depending on heart rate). Both cine images and late enhancement images were obtained in the same short-axis views (10 to 14 contiguous slices) and 4-, 2-, and 3-chamber views. Late enhancement was performed 10 to 15 min after a total injection of 0.2 mmol/kg gadodiamide (Omniscan, GE Healthcare, Oslo, Norway).

Electrophysiological Study

Electrophysiologists were blinded to the results of ceMRI. The electrophysiological study has been described elsewhere (4). Briefly, once written informed consent was obtained, VT patients underwent an electrophysiological study in the post-absorptive state 4 ± 7 days after ceMRI. At least 2 quadripolar catheters were placed in the bundle of His and right ventricular apex or right ventricular outflow tract.

Left ventricle mapping. Detailed endocardial mapping was performed during sinus rhythm or right ventricular apex pacing at 600 ms. Mapping and ablation was performed using the CARTO magnetic mapping system (Biosense, Inc., Diamond Bar, California) with the Navistar Thermocool catheter (Biosense, Inc.). To define the presence of CC, several sites were explored to obtain a fill threshold of 10 mm in the zone of interest within the low voltage area, so that the distance between mapped sites was ≤1 cm.

RF ablation procedure. Radiofrequency (RF) ablation was performed with a 550-kHz RF Stockert-Cordis generator. The RF energy was delivered in a temperature-controlled mode for 60 to 120 s at each ablation site with a maximal temperature target of 45°C and 35 to 40 W of maximum power delivered.

The end points of the procedure were as follows: 1) suppression of induced clinical VT; and/or 2) disappearance of clinical VT-related CC or electrograms with delayed components in those patients with unmappable VT. Heparin was infused throughout the procedure. An ICD was implanted in all patients after the procedure.

Data Analysis

The MRI data were analyzed by 2 investigators (E.P.D. and V.C.), who were blinded to VT morphology, electrophysiology study results, and participant group (SMVT or control). Cine and late enhancement images were analyzed offline in DICOM (Digital Imaging and Communications in Medicine) format with specialized software (QMass MR version 7.0, MEDIS, the Netherlands). Left ventricular end-diastolic and end-systolic volumes were assessed according to Simpson's rule, and the ejection fraction was calculated. Left ventricular mass was calculated by subtracting the endocardial volume from the epicardial volume at end diastole and then multiplying by the tissue density (1.05 g/ml).

Late gadolinium-enhanced images were used for infarct characterization. We used SI thresholds to quantify 2 different areas within the infarct zone: 1) a core area defined by an SI >3 SD higher than remote normal myocardium; and 2) heterogeneous tissue (i.e., gray zone) defined by an SI of between 2 and 3 SDs (8,9).

Identification of HT channels by MRI. The HT channels in the ventricular wall were identified and defined within the hyperenhanced region as follows:

1. Computer-assisted visual identification of HT: short-axis slices were examined when the SI threshold was set at >2 SD and at >3 SD higher than remote normal myocardium. A subtraction image of the difference between both images was obtained by means of a custom-developed Java program, based on JAI (Java Advanced Imaging application programming interface, Sun Microsystems, Oracle Corp., Redwood Shores, California) that allows imaging arithmetic operations (Fig. 1).
2. Architecture of HT: short-axis consecutive subtraction image slices were evaluated to determine the continuity of the HT and its connections to normal myocardium.

An HT channel was defined as a corridor of HT in consecutives slices surrounded by scar and connected to normal myocardium by at least one side. An HT channel was characterized by the following: 1) depth in the ventricular wall (endocardium, mesocardium, and epicardium); 2) segment location—for this purpose, the ventricle was divided into 12 myocardial segments, as defined by Josephson et al. (11); and 3) channel orientation—parallel or perpendicular to the mitral valve. The presence of a channel was only accepted if both investigators independently agreed on the depth, location, and orientation of the channel.

Endocardial SI mapping. SI mapping was designed to assist in the ablation procedure based on the hypothesis that SI mapping could reproduce endocardial voltage mapping. As endocardial voltage mapping cannot record mesocardial or subepicardial electrical activity to maintain the parallelism between SI and voltage mapping the myocardial wall was divided into 2 equal parts: subendocardium and subepicardium. The averaged SI of the inner half of the wall (subendocardial tissue) was projected onto a 3D endocardial shell reconstruction of the left ventricle that was color-coded to provide information on subendocardial signal intensity. For this process, the left ventricular endocardial/epicardial contours were manually defined on contiguous short-axis slices using QMass MR version 7.0 and imported into our tool. A 3D endocardial reconstruction was computed offline from an image volume that integrates the short-axis, 4- and 2-chamber ceMRI views using custom software developed in the MATLAB environment (Mathworks, Natick, Massachusetts). The 3D visualization interface was implemented in Java (Sun Microsystems) using VTK (Kitware, Clifton Park, New York) visualization algorithms. In the endocardial shell, a channel was defined as a corridor of continuous tissue differentiated by a lower SI from the surrounding scar tissue and connected to normal myocardium by at least 1 connection (Fig. 2). We differen-

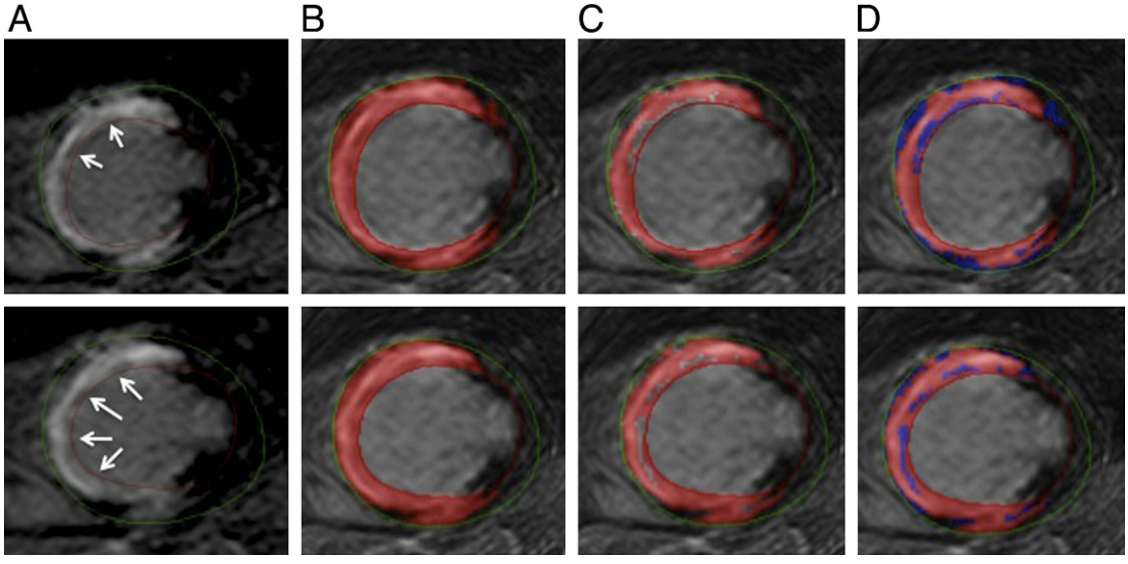

Figure 1 ceMRI Identification of HT in the Infarct Zone

Two short-axis slices of an anteroseptal myocardial infarction in a patient from the sustained monomorphic ventricular tachycardia group: **(A)** the unprocessed infarct zone (**arrows** show the heterogeneous tissue), **(B)** area with signal intensity >2 SD, **(C)** area with signal intensity >3 SD (the core of the scarred area), and **(D)** the differences between **B** and **C** (signal intensity >2 SD and ≤3 SD): heterogeneous tissue is shown in **blue.** ceMRI = contrast-enhanced magnetic resonance imaging; HT = heterogeneous tissue.

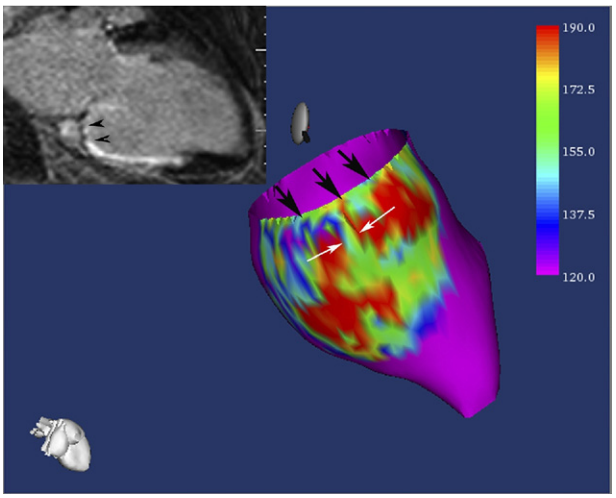

Figure 2 **Endocardial SI Mapping From a Patient With a Septal and an Inferior Scar**

This figure shows the average signal intensity (SI) of the subendocardial tissue projected onto a 3-dimensional endocardial shell reconstruction of the left ventricle. The color range provides information on subendocardial SI: the **red** area represents SI greater than the minimal SI in the core of the scar; the **magenta** area represents normal myocardium (SI less than SI peak in the normal myocardium) and the area between these extremes is the heterogeneous tissue. Notice 2 corridors of continuous tissue differentiated from the surrounding scar tissue by a lower SI: the first is located between the mitral valve and the inferior scars (submitral channel, **black arrows**) and the second is between the septal and inferior scars and perpendicular to the mitral valve **(white arrows)**. In the left superior corner, a long-axis magnetic resonance imaging view is shown, and the **black arrowheads** mark the heterogeneous tissue channel that corresponds to the submitral SI channel.

tiated incomplete and complete channels that were connected to normal myocardium on 1 or 2 sides respectively.

Endocardial voltage mapping. An investigator (L.A.) who was blinded to the MRI data analyzed the voltage maps. Fifteen voltage maps were analyzed for each patient. Voltage maps were displayed using 1.5/1.51 to 0.10/0.11 mV in steps of 0.1 mV as the lower and upper limits in the color range; any electrogram above the upper limit was depicted in magenta and any electrogram below or equal to the lower limit in red. An endocardial slow CC and the activation sequence within the channel were defined as referred (4). Electrograms with an isolated delayed component were also tagged in the scar (12).

Comparison of SI and voltage maps in the SMVT group. Although merging was not performed during the EP study, SI and voltage maps were analyzed off-line. To compare the location of the channel detected by endocardial SI mapping and the CC detected by voltage mapping, we proceeded as follows:

1. As color-coded SI maps could not be directly imported in CARTO, the color range of the SI map was grouped into 3 discrete levels corresponding to: 1) healthy tissue defined by SI less than SI peak in normal myocardium (magenta); 2) core scar defined by SI greater than minimal SI in core scar (red); and 3) heterogeneous tissue in between those extremes (green). The 3D surface map data were then converted to volumetric DICOM data corresponding to each surface and imported into the CARTO Merge software (Biosense Webster) for synchronized visualization with the voltage map. Three-dimensional registration of the MRI surface data and the electroanatomic mapping data was initially accomplished using the left ventricular apex and the mitral annulus of both MRI data and electroanatomic mapping data.
2. The left ventricle was divided into 12 segments (11). To define the orientation, the channels were classified as parallel or perpendicular to the mitral annulus. Channels bordered by the scar and the mitral annulus were termed *submitral channels*.
3. To state that a CC and an SI channel represented the same structure, coincidence in wall/segment location and orientation was required.

Relationship between VT and CC. We assumed a relationship between a specific CC and a clinical or induced VT when the following criteria were met:

Table 1 **Baseline Characteristics**

	SMVT Group	Control Group	p Value
Age, yrs	66 ± 8	64 ± 11	NS
Sex (male/female)	15/3	15/3	NS
EDV	256 ± 86	222 ± 56	0.18
ESV	184 ± 88	152 ± 56	0.19
LVEF	32 ± 10	33 ± 9	NS
NYHA functional class I, II, and III	9/6/3	8/7/3	NS
Infarct location inferior vs. noninferior	14/4	14/4	NS
ACE inhibitors or ARBs	14	12	NS
Beta-blockers	16	13	NS
Amiodarone	3	0	NS
Left bundle branch block	5	4	NS
Atrial fibrillation	2	2	NS

ACE = angiotensin-converting enzyme; ARB = angiotensin receptor blocker; EDV = end-diastolic volume; ESV = end-systolic volume; LVEF = left ventricular ejection fraction; NS = not significant; NYHA = New York Heart Association; SMVT = sustained monomorphic ventricular tachycardia.

Table 2 **MRI Data**

	Study Group	Control Group	p Value
Myocardial mass, g	183 ± 47	158 ± 43	0.10
Necrotic mass, g	49 ± 24	39 ± 16	0.10
Mass >3 SD	73 ± 38	52 ± 28	0.07
Mass >2 SD, g	89 ± 40	68 ± 32	0.08
Mass >2 SD and <3 SD, g (heterogeneous tissue)	16 ± 6	15 ± 7	NS
Heterogeneous tissue channel, % (of patients)	88%	33%	0.0006
Endocardial heterogeneous tissue channel, % (of patients)	83%	22%	0.0006
SI channel (% of patients)	94%	55%	0.01

MRI = magnetic resonance imaging; other abbreviations as in Table 1.

1. Noninducible VT: pace mapping reproducing the clinical QRS VT and a stimulus to QRS interval >50 ms.
2. Inducible poorly tolerated VT: presence of a pre-systolic or mid-diastolic electrogram and a difference ≤30 ms between the electrogram-QRS interval on VT and stimulus to QRS when the preceding pace mapping was similar.
3. Well-tolerated VT: the presence of a pre-systolic or mid-diastolic electrogram, concealed entrainment, and a first post-pacing interval-VT cycle length difference <30 ms. In the cases that RF pulses terminated the VT, we considered the channel to be VT-related when the successful ablation site was less than 5 mm from any part of the channel.

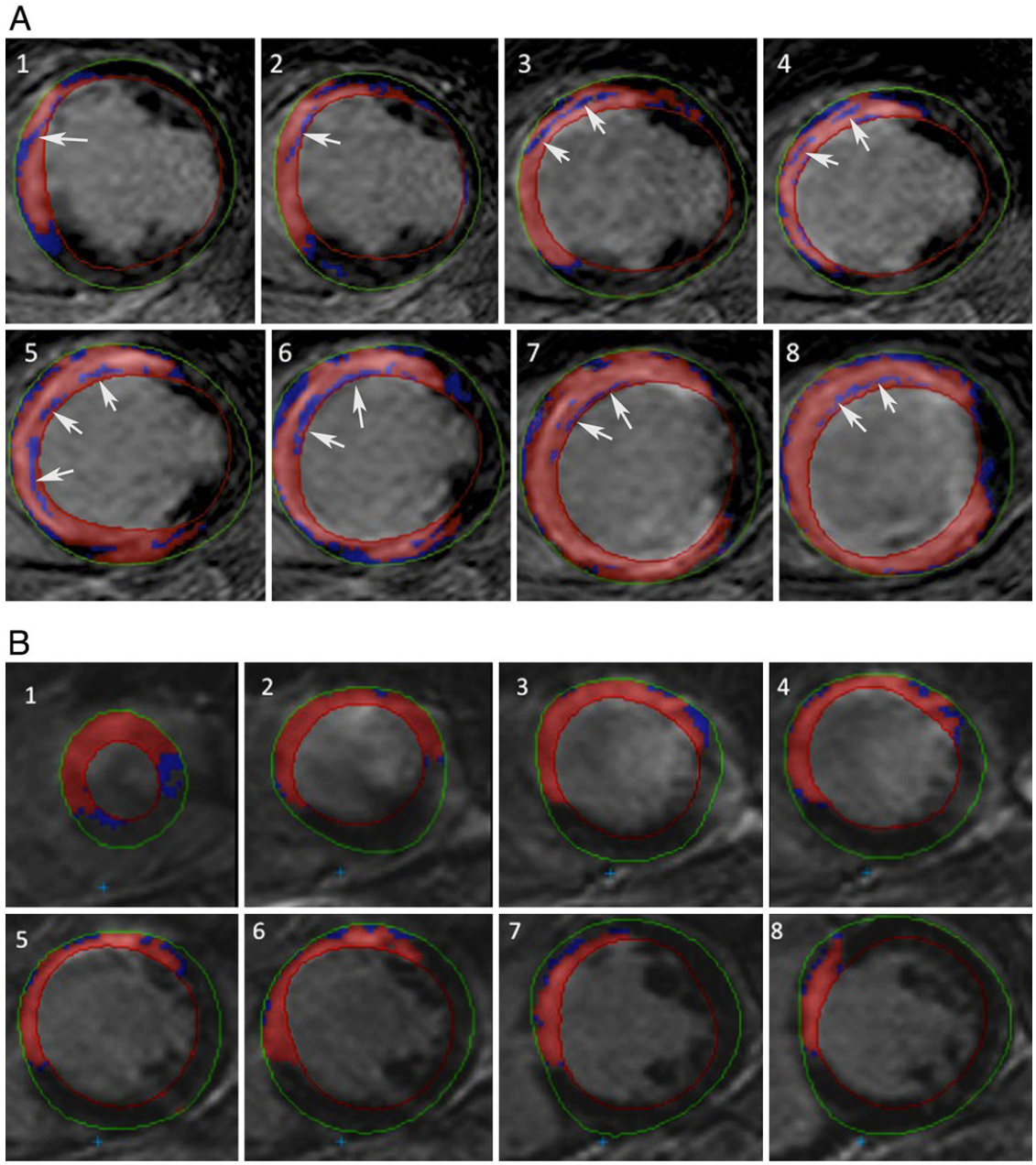

Figure 3 **Short-Axis Slices of an Anteroseptal Myocardial Infarction in Patients From the SMVT and Control Groups**

(A) Short-axis slices of an anteroseptal myocardial infarction in a patient from the sustained monomorphic ventricular tachycardia (SMVT) group. Notice the continuity of the heterogeneous tissue in the successive short-axis slices creating a corridor/channel that extends from the base to the apex. In **frames 1 and 2,** the heterogeneous tissue is located in the subendocardium; in **frames 3 and 4,** the heterogeneous tissue moves to the subepicardium; and in **frames 5, 6, 7, and 8,** it has moved back to the subendocardium. **(B)** The short-axis slices of an anteroseptal myocardial infarction in a patient from the control group. Despite the absence of endocardial heterogeneous tissue, a heterogeneous tissue channel was observed in the epicardium.

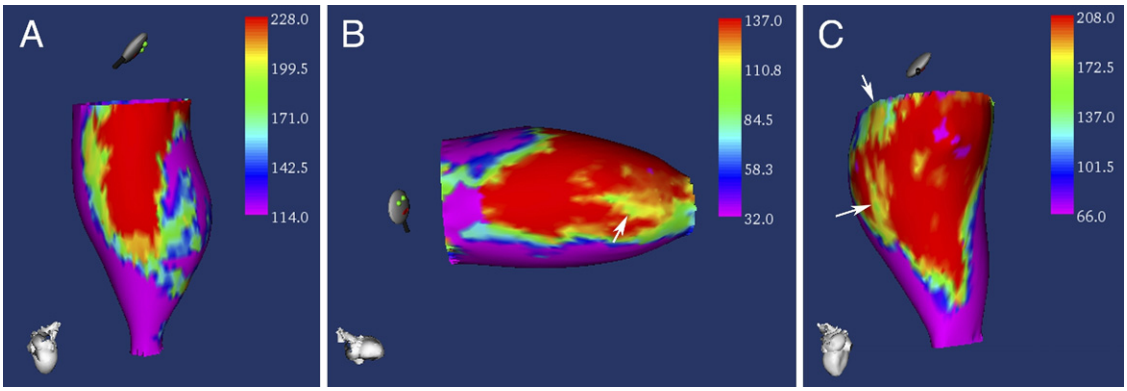

Figure 4 **Endocardial SI Mapping From 3 Different Patients of the Control Group**

The color range provides information on subendocardial signal intensity as in Figure 2. Notice the absence of signal intensity (SI) channels **(A)**, and short incomplete channels **(white arrows)** related to an anteroseptal infarction **(B)** and inferior infarction **(C)**.

Statistical Analysis

Values are expressed as mean ± SD. Comparisons were made using the *t* test, paired *t* test, and the Fisher exact test. Linear regression was used to estimate the relation between infarct mass and scar extension. A p value of <0.05 was considered significant.

Table 3 **Segment Location and Orientation of CC and SI Channels**

		Endocardial Voltage Mapping			Endocardial SI Mapping	
Patient #	Infarct Location	Channel n° and Segment Location	Orientation	VT-Related	Channel n° and Segment Location	Orientation
1	Ant	1: 3, 2, 1	Per		1: 3, 2, 1	Per
2	Inf	1: 6, 8	Para	+	1: 6, 8	Para
		2: 3, 5, 7	Para		2: 3, 5, 7	Para
3	Inf	1: 5, 6	Per	+	1: 5, 6	Per
4	Inf	1: 4, 6, 8	Para	+	1: 4, 6, 8	Para
5	Inf-Lat	1: 6, 8	Para		1: 6, 8	Para
		2: 6, 8, 5, 7	Per	+	2: 6, 8, 5, 7	Per
6	Ant					
7	Inf	1: 6	Para		1: 6	Para
		2: 6, 5	Para	+	2: 6, 5	Para
		3: 4, 6	Per		3: 4, 6	Per
8	Inf	1: 4, 6	Per		1: 4, 6	Per
9	Inf	1: 6, 8	Para	+	1: 6, 8	Para
10	Inf	1: 5, 6	Para	+	1: 5, 6	Para
11	Inf	1: 6	Para	+	1: 6	Para
12	Inf-Lat	1: 6	1: Para	+	1: 6	1: Para
		2: 5, 7, 6, 8	2: Per		2: 5, 7, 6, 8	2: Per
13	Inf	1: 6	Para	+	1: 6	Para
14	Ant	1–2	Para	+	1–2	Para
15	Inf	1: 6, 8	Para	+	1: 6, 8	Para
		2: 5, 6	Para		2: 5, 6	Para
		3: 4, 6	Per		3: 4, 6	Per
16	Ant	1: 2, 3	Para	+	1: 2, 3	Para
		2: 2, 3, 4	Per		2: 2, 3, 4	Per
17	Inf-Lat	1: 6, 8	Para	+	1: 6, 8	Para
		2: 4, 6	Per		2: 4, 6	Per
18	Inf	1: 6	Para	+	1: 6	Para

Segment locations from Josephson (11), used with permission.

Ant = anterior; CC = conduction channels; Inf = inferior; Lat = lateral; Para = parallel to mitral annulus; Per = perpendicular to mitral annulus; SI = signal intensity; + = ventricular tachycardia-related channels.

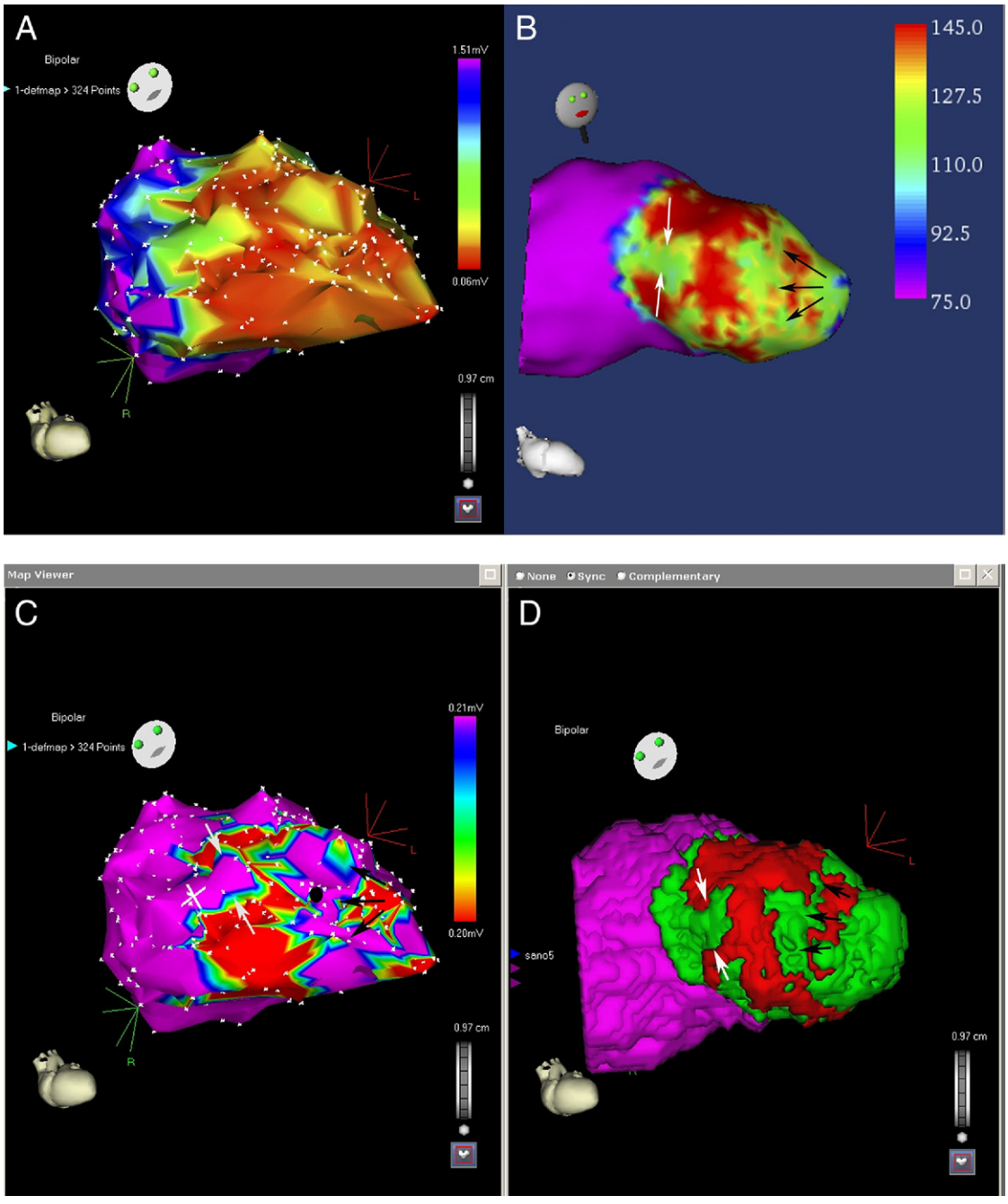

Figure 5 **Maps of Anterior Infarct, Relation of Voltage and SI Mapping, and Morphology of Induced VT**

(Top panel) Endocardial voltage **(A)** and subendocardial signal intensity **(B)** maps of an anterior infarct showing the similarity of scar from the patient shown in Figure 3A. **(A)** The voltage map shows the extension of the scar when the voltage scar definition was set >1.5 mV. **(B)** The signal intensity map is consistent with the magnetic resonance imaging short-axis view shown in Figure 3A. The channel that runs parallel to the mitral annulus between segments 2 and 3 **(black arrows)** coincides with the heterogeneous tissue channel in frames 5 and 6 in Figure 3A. The second channel, perpendicular to the mitral annulus is in segment 3 **(white arrow)**, this channel corresponds with the heterogeneous tissue channel in frames 1 and 2. The continuity of the signal-intensity channel is interrupted when the heterogeneous tissue channel (frame 3) moves to the epicardium. Then it moves back to the endocardium and joins the first channel. **(Middle panel)** Relation of voltage and signal-intensity mapping. The processed signal-intensity map was imported and recreated with CARTO Merge for comparison with a voltage map. The channels observed in the voltage map **(C)** in which the scar voltage definition was set at 0.2 mV are also identified in the signal-intensity maps **(D)**.

Continued on next page

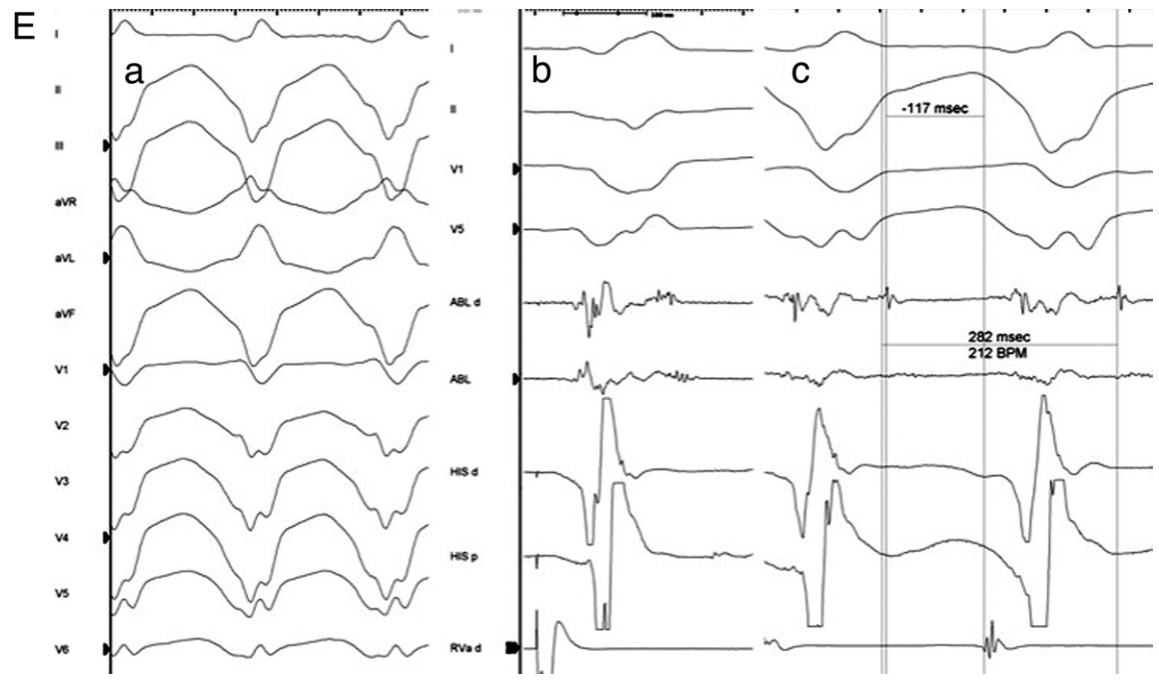

Figure 5 Continued

(E) (a) Morphology of induced ventricular tachycardia (identical to clinical tachycardia): 282 ms. **(b)** Electrograms recorded at the **black dot** site in the voltage map from Figure 4 middle panel. This electrogram was recorded during right ventricular apex pacing and showed an isolated delayed component. After ventricular tachycardia induction, the electrogram became mid-diastolic **(c)**. Ablation at this site terminated the ventricular tachycardia. VT = ventricular tachycardia; other abbreviations as in Figure 2.

Results

Baseline characteristics. The baseline characteristics of both groups are shown in Table 1. No differences were observed between the groups and no control patients were on antiarrhythmic drugs. The mean VT cycle length of the SMVT group was 364 ± 67 ms; in 6 cases, the cycle length was ≤320 ms.

Comparison of ceMRI between SMVT and control groups. Despite the fact that no differences were observed between the groups in left ventricular ejection fraction or necrotic mass (Table 2), HT channels were more common in the SMVT group (88% vs. 33% of patients, $p < 0.005$, Fisher exact test). Twenty-two HT channels (21 partially or totally in the subendocardium) were identified in 16 SMVT patients (Fig. 3A); in the control group, only 6 channels (4 in the endocardium) in 6 patients were detected (Fig. 3B). Endocardial SI mapping detected 26 channels in 17 patients of the SMVT group and 13 in 10 patients of the control group (94% vs. 55% of patients, $p < 0.01$, Fisher exact test). In the SMVT group only 4 of the 26 detected channels were incomplete (connected to normal myocardium by 1 sides), whereas in the control group 6 of 13 (15% vs. 46%, $p < 0.05$). In the SMVT group 17 of 18 patients had at least a complete channel, in the control group a complete channel was absent in 13 of 18 patients (Fig. 4).

Voltage and SI mapping in the SMVT group. There was a significant relation between infarct mass (SI >2 SD) and scar extension defined by <1.5 mV ($R^2 = 0.4$, $p < 0.009$), but not between dense scar (<0.5 mV) and core scar (SI >3 SD). Twenty-six slow CC were observed in 17 of 18 patients (1 to 3 per patient). Multicomponent electrograms were recorded in the inner part of all channels, and the activation time of the latest component was longer than the latest component of the electrograms recorded at the entrance (167 ± 33 ms vs. 118 ± 28 ms, $p < 0.0001$). Voltage tended to be higher at the entrance electrograms (1.3 ± 1.1 vs. 0.7 ± 0.5, $p < 0.07$). All 26 SI channels coincided in location and orientation with a corresponding CC in the voltage maps (Table 3). The SI channels were identified independently of the infarct location (Figs. 5 and 6). SI mapping detected the endocardial trajectory of HT channels but not the mesoepicardial trajectory (Fig. 5).

Relationship between SMVT and CC. Fifteen CC identified in 15 patients by endocardial voltage mapping were related to clinical VT. All these channels had a corresponding SI channel. Clinical VT was induced, and mid-diastolic electrograms were recorded in the inner part of the CC in 10 patients (Fig. 5). In the remaining 5 patients in whom clinical VT was not induced, the channel was related to the clinical VT by pace mapping. In total, an endocardial SI channel related to clinical VT was identified in 83% of

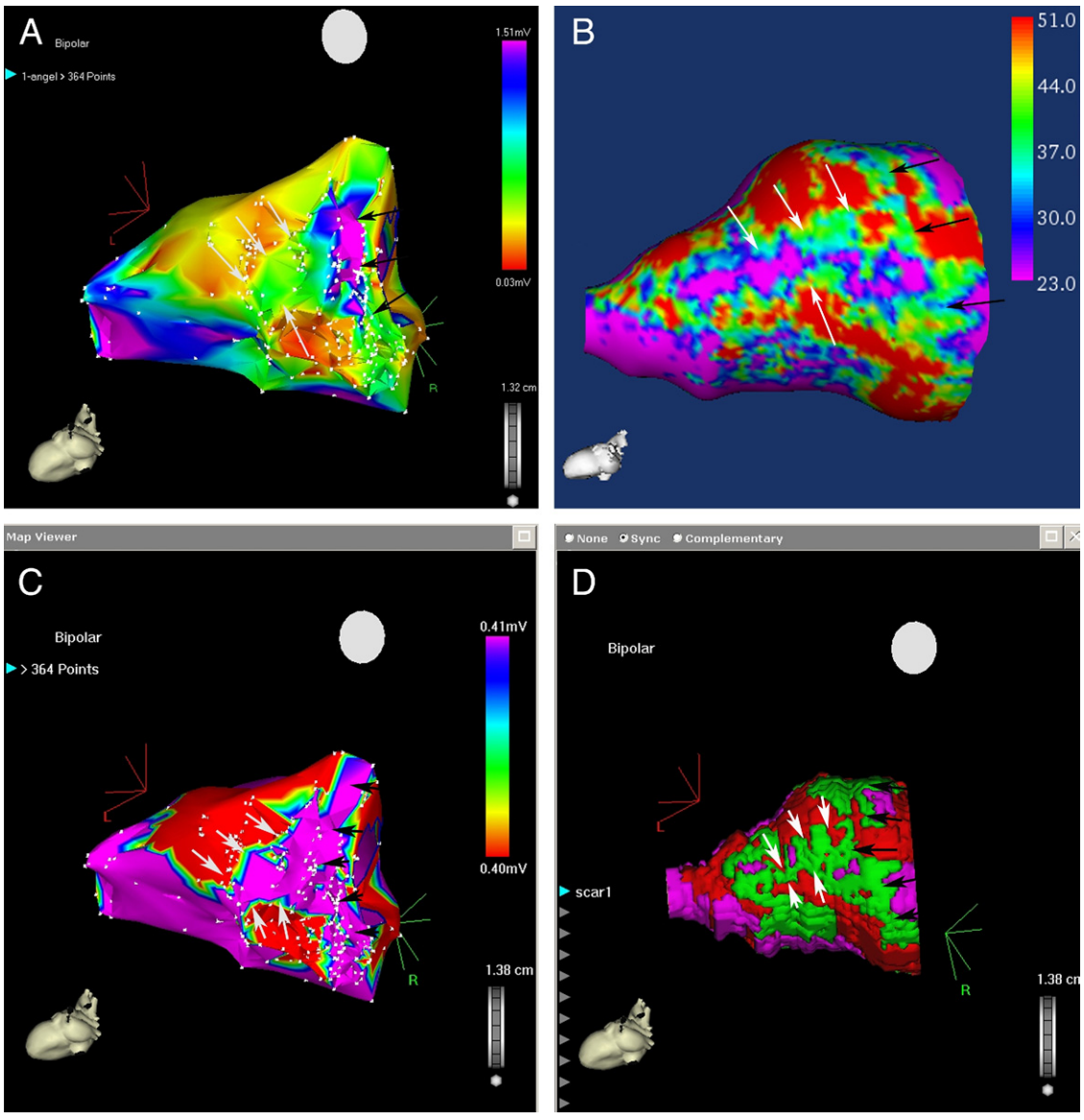

Figure 6 **Maps From an Inferior and Lateral Infarction and Relation of Voltage and SI Mapping**

(Top panels) Endocardial voltage **(A)** and subendocardial SI **(B)** maps from an inferior and lateral infarction. **(A)** The voltage map shows the extension of the scar when the voltage scar definition was set <1.5 mV. **(B)** The SI map shows a channel that runs parallel to the mitral annulus from segments 6 and 10 **(black arrows)** and a second channel perpendicular to the mitral annulus between segments 6 to 8 and 5 to 7 **(white arrows). (Bottom panels)** Relation of voltage and signal-intensity mapping. The processed SI map was imported and recreated with CARTO Merge for comparison with a voltage map. The channels observed in the voltage map **(C)** in which the scar voltage definition was set at 0.4 mV are also identified in the SI maps **(D).** Abbreviations as in Figure 2.

patients. In 3 patients, no relationship was established between any VT and a CC. In 1 patient, no CC or SI channels were identified (Patient #6, Table 3).

RF ablation results. A mean of 20 ± 5 RF lesions were applied per patient. Radiofrequency pulses were delivered over electrograms located in all SMVT-related CC in 15 patients. In 10 channels (10 patients), the ablation was performed during tachycardia, which terminated in all cases. In the remaining 5 patients in whom VT-related channels were identified, lesions were delivered during sinus rhythm because of noninducibility of documented VT. Additional RF pulses were delivered over all electrograms with isolated delayed components.

In the remaining 3 patients in whom no relation between CC and VT could be established, ablation was anatomically guided toward VT-related electrograms with isolated delayed components (12).

After ablation, previously inducible VT became noninducible in all but 2 patients, ventricular fibrillation was induced in 2 patients, and a fast nonclinical VT was induced

in 4 patients. No complications were observed during the procedure. After the RF ablation procedure, all patients were discharged with an ICD.

Follow-up. The mean follow-up was 12 ± 6 months in the SMVT group and 14 ± 5 months in the control group. One SMVT patient died of cancer and another of heart failure; 4 patients had SMVT recurrences. In the control group, 3 patients died: 2 of cancer and 1 of stroke. In the control group, 4 patients received an ICD for primary prevention of sudden cardiac death, 2 patients had an HT channel, and 1 of these had VT episodes.

Discussion

Main findings. This study provides significant new information on SMVT substrate: channels of HT are more commonly identified in SMVT than in control patients, and the CC detected by endocardial voltage mapping can be identified by 3D SI mapping.

Heterogeneous tissue and SMVT substrate. Haqqani et al. (13) have reported that, in ischemic cardiomyopathy patients, conducting channels within dense scar and adjacent to the mitral annulus were more frequently observed in SMVT patients than in stable control patients despite similar left ventricular parameters. We used a noninvasive approach to make a similar observation, namely, that HT and SI channels are more frequently observed in patients with clinical SMVT than in control patients and that these channels were mainly located in the endocardium. Schmidt et al. (10) have indirectly related tissue heterogeneity and VT substrate, showing that HT mass was associated with inducibility for monomorphic VT. Although we found that HT mass was similar in SMVT and control patients, both studies support the relation between HT and VT substrate. The difference is probably due to the fact that each study analyzes a different type of tachycardia (inducible vs. spontaneous) with a different cycle length (231 ± 37 ms vs. 364 ± 67 ms).

Comparison of voltage mapping and SI mapping. Scar extension by voltage mapping and ceMRI has been compared elsewhere (14), and some discrepancies have been observed, mainly due to poor wall/catheter contact, or far-field influences from normal myocardium that may lead to underestimation of endocardial scar dimensions on endocardial voltage maps. Despite these limitations, we observed a significant relationship between the infarct mass (SI >2 SD) and scar extension (<1.5 mV), as well as a strong similarity in CC and SI channels with regard to location and orientation. Channel similarity despite scar differences could be explained by the fact that far-field influences do not seem to affect characterization of CC. The surrounding scar ameliorates far-field influences, and CC do not affect the surrounding scar areas because of the reduced amount of myocytes embedded in these zones.

Prior studies. Although some authors have analyzed ceMRI in VT patients, a clear understanding of VT substrate in the scar has not been established. Codreanu et al. (14) compared ceMRI data in post-infarction VT patients for whom electroanatomic mapping data were available, but they did not provide data on the VT substrate. Desjardins et al. (15) showed that critical sites of post-infarction arrhythmias were confined to areas of high SI, but the VT substrate inside the scar was also not differentiated. Our study adds further information by describing the presence of HT channels in the scar and a methodology for SI mapping that identifies endocardial VT substrate in the same way as voltage mapping.

Study limitations. The main limitation of our study is the low number of patients included due to restrictions affecting the use of MRI in ICD patients. Although most patients had an inferior infarction, as previously reported in SMVT patients (16), these patients were not specifically selected, as consecutive patients with infarcts at different locations were included. To maintain blindness to MRI results, SI maps were not merged in CARTO online; therefore, evidence of perfect correlation between CC and SI channels is not provided, nevertheless offline synchronic comparison with CARTO Merge proves similar location and orientation of SI channels and CC. Although no activation mapping during tachycardia was systematically obtained, the consistency in the relationship between the SMVT circuit and CC is supported by pacing, activation mapping, and successful ablation sites. Only a few SMVTs of <320 ms were included. In the control group, 33% of patients had an HT channel, but because no electrophysiological study was performed, we cannot state explicitly that they were related to an SMVT.

Clinical implications. The HT and SI channels could help to identify patients at risk of SMVT, and this information could be useful to identify primary prevention patients in whom prophylactic substrate ablation could reduce ICD discharges (17). Signal-intensity mapping could identify CC and facilitate ablation procedures by merging into 3D mapping systems (18).

Acknowledgments

The authors thank Juan Felipe Cerezo for software development, Thomas O'Boyle for language revision, and Antonio Moratalla for technical assistance.

Reprint requests and correspondence: Dr. Ángel Arenal, Unidad de Arritmias, Servicio de Cardiología, Hospital General Universitario Gregorio Marañón, C/Dr. Esquerdo, 46 28007 Madrid, Spain. E-mail: arenal@secardiologia.es.

REFERENCES

1. de Bakker JM, van Capelle FJ, Janse MJ, et al. Reentry as a cause of ventricular tachycardia in patients with chronic ischemic heart disease: electrophysiologic and anatomic correlation. Circulation 1988;77:589–606.
2. de Bakker JM, Coronel R, Tasseron S, et al. Ventricular tachycardia in the infarcted Langendorff-perfused human heart: role of the arrangement of surviving cardiac fibers. J Am Coll Cardiol 1990;15:1594–607.

3. Soejima K, Stevenson WG, Maisel WH, Sapp JL, Epstein LM. Electrically unexcitable scar mapping based on pacing threshold for identification of the reentry circuit isthmus: feasibility for guiding ventricular tachycardia ablation. Circulation 2002;106:1678–83.
4. Arenal A, del Castillo S, Gonzalez-Torrecilla E, et al. Tachycardia-related channel in the scar tissue in patients with sustained monomorphic ventricular tachycardias: influence of the voltage scar definition. Circulation 2004;110:2568–74.
5. Hsia HH, Lin D, Sauer WH, Callans DJ, Marchlinski FE. Anatomic characterization of endocardial substrate for hemodynamically stable reentrant ventricular tachycardia: identification of endocardial conducting channels. Heart Rhythm 2006;3:503–12.
6. Amado LC, Gerber BL, Gupta SN, et al. Accurate and objective infarct sizing by contrast-enhanced magnetic resonance imaging in a canine myocardial infarction model. J Am Coll Cardiol 2004;44:2383–9.
7. Kim RJ, Albert TSE, Wible JH, et al., for the Gadoversetamide Myocardial Infarction Imaging Investigators. Performance of delayed-enhancement magnetic resonance imaging with gadoversetamide contrast for the detection and assessment of myocardial infarction: an international, multicenter, double-blinded, randomized trial. Circulation 2008;117:629–37.
8. Bello D, Fieno DS, Kim RJ, et al. Infarct morphology identifies patients with substrate for sustained ventricular tachycardia. J Am Coll Cardiol 2005;45:1104–8.
9. Yan AT, Shayne AJ, Brown KA, et al. Characterization of the peri-infarct zone by contrast-enhanced cardiac magnetic resonance imaging is a powerful predictor of post-myocardial infarction mortality. Circulation 2006;114:32–9.
10. Schmidt A, Azevedo CF, Cheng A, et al. Infarct tissue heterogeneity by magnetic resonance imaging identifies enhanced cardiac arrhythmia susceptibility in patients with left ventricular dysfunction. Circulation 2007;115:2006–14.
11. Josephson ME. Clinical Cardiac Electrophysiology. 3rd edition. Philadelphia, PA: Lippincott Williams & Wilkins, 2002.
12. Arenal A, Glez-Torrecilla E, Ortiz M, et al. Ablation of electrograms with an isolated, delayed component as treatment of unmappable monomorphic ventricular tachycardias in patients with structural heart disease. J Am Coll Cardiol 2003;41:81–92.
13. Haqqani HM, Kalman JM, Roberts-Thomson KC, et al. Fundamental differences in electrophysiologic and electroanatomic substrate between ischemic cardiomyopathy patients with and without clinical ventricular tachycardia. J Am Coll Cardiol 2009;54;166–73.
14. Codreanu A, Odille F, Aliot E, et al. Electroanatomic characterization of post-infarct scars: comparison with 3-dimensional myocardial scar reconstruction based on magnetic resonance imaging. J Am Coll Cardiol 2008;52:839–42.
15. Desjardins B, Crawford T, Good E, et al. Infarct architecture and characteristics on delayed enhanced magnetic resonance imaging and electroanatomic mapping in patients with postinfarction ventricular arrhythmia. Heart Rhythm 2009;6:644–51.
16. Stevenson WG, Wilber DJ, Natale A, et al., Multicenter Thermacool VT Ablation Trial Investigators. Irrigated radiofrequency catheter ablation guided by electroanatomic mapping for recurrent ventricular tachycardia after myocardial infarction: the multicenter thermocool ventricular tachycardia ablation trial. Circulation 2008;118:2773–82.
17. Reddy VY, Reynolds MR, Neuzil P, et al. Prophylactic catheter ablation for the prevention of defibrillator therapy. N Engl J Med 2007;357:2657–65.
18. Reddy VY, Malchano ZJ, Holmvang G, et al. Integration of cardiac magnetic resonance imaging with three-dimensional electroanatomic mapping to guide left ventricular catheter manipulation feasibility in a porcine model of healed myocardial infarction. J Am Coll Cardiol 2004;44:2202–13.

Key Words: ablation ■ heterogeneous imaging ■ magnetic resonance imaging ■ ventricular tachycardia.